Article

A New 3D Chaotic Attractor in Gene Regulatory Network

Olga Kozlovska [1,†], Felix Sadyrbaev [2,†] and Inna Samuilik [1,*,†]

1   Institute of Applied Mathematics, Riga Technical University, Zunda Embankment 10, LV-1048 Riga, Latvia; olga.kozlovska@rtu.lv
2   Institute of Mathematics and Computer Science, University of Latvia, Rainis Boulevard 29, LV-1459 Riga, Latvia; felix@latnet.lv
*   Correspondence: inna.samuilika@rtu.lv
†   These authors contributed equally to this work.

Abstract: This paper introduces a new 3D chaotic attractor in a gene regulatory network. The proposed model has eighteen parameters. Formulas for characteristic numbers of critical points for three-dimensional systems were considered. We show that the three equilibrium points of the new chaotic 3D system are unstable and deduce that the three-dimensional system exhibits chaotic behavior. The possible outcomes of this 3D model were compared with the results of the Chua circuit. The bifurcation structures of the proposed 3D system are investigated numerically, showing periodic solutions and chaotic solutions. Lyapunov exponents and Kaplan-Yorke dimension are calculated. For calculations, the Wolfram Mathematica is used.

Keywords: chaos theory; gene regulatory network; Chua circuit; 3D chaotic attractor

MSC: 34C25; 34D45; 92-08; 92-10

1. Introduction

Deterministic chaos of nonlinear dynamic systems is not chaos, usually understood as complete disorganization and randomness of events; modern ideas about chaos are to some extent closer to the original ancient Greek ones: "chaos" like a boundless disordered mass from which everything that exists arose.

Chaos theory is a branch of science that deals with complex systems and their behavior. Meteorologist Edward Lorenz made a major contribution to chaos theory [1]. During the 1960s, Lorenz developed a computer program that simulated the motion of air masses within the Earth's atmosphere [2]. The Lorenz model demonstrated a susceptibility to initial conditions [3]. Tiny variations in input data resulted in significant discrepancies in outcomes over time. This reliance on the starting conditions was termed chaos. Lorenz coined a famous feature of chaos called the "butterfly effect", the notion that a butterfly stirring the air in Hong Kong today can transform storm systems in New York next month [4]. After Lorenz's studies, many chaotic systems have been presented to the literature Rossler system [5], Chen system [6], LU system [7], Sprott system [8] and others. For a long time, chaos theory was considered a kind of mathematical abstraction that had no confirmation in real conditions. Now it has applications in various scientific disciplines, including physics [9], biology (in the study of uneven heart rate and an uneven number of diseases) [10], meteorology, economics [11], finance [12], geology [13], computer science, engineering, algorithmic trading, politics [14], population dynamics [15], robotics [16], philosophy [17] and mathematics.

Chaos is a complex phenomenon defying easy classification or identification. Although there exists no universally accepted definition for chaos, the solutions of chaotic systems typically exhibit the characteristics [18].

Characteristics of chaos:

- chaotic behavior is characterized by the presence of an attractor to which all nearby solutions tend to converge over time, provided there is ample time for the process [19];
- a common feature of chaotic solutions lies in the geometric structure of their attractors. These attractors often exhibit intricate and unconventional shapes, characterized by a twisted and "strange" appearance. This strangeness is indicative of a fractional (fractal) dimension, although it's important to note that this isn't always the case [19];
- sensitivity to initial conditions [18].

Nonlinear ordinary differential equations are the most widespread formalism for modeling genetic regulatory networks [20]. The main contributions of the present study are summarized as follows:

- formulas for characteristic numbers of critical points for three-dimensional systems were considered;
- the new chaotic attractor is obtained;
- the three-dimensional system (7) can have attractors of various kinds;
- the irregular behavior of solutions near the chaotic attractor is conceivable and may manifest within a narrow parameter range.

2. Materials and Methods

2.1. Chua Circuit

Leon O. Chua is a renowned electrical engineer and computer scientist who has made significant contributions to the fields of electronics, circuits, and nonlinear science. He was born on 28 June 1936, in Manila, Philippines. He is a professor in the Electrical Engineering and Computer Sciences department at the University of California, Berkeley. The professor's scientific projects are related to cellular neural network technologies, bifurcation theory, nonlinear dynamics, and chaos theory. Leon Chua aimed to show that it was possible to create chaos. For this purpose, in 1983 he assembled an electrical circuit [21]. It is a simple oscillatory circuit demonstrating a series of bifurcations and a transition to chaos. In the simple case, Chua's equations can be written in the following form:

$$\begin{cases} \dfrac{dx}{d\tau} = \alpha(y - x - f(x)), \\[2mm] \dfrac{dy}{d\tau} = x - y + z, \\[2mm] \dfrac{dz}{d\tau} = -\beta y, \end{cases} \tag{1}$$

$$f(x) = \begin{cases} bx + a - b, & x \geq 1, \\ ax, & |x| \leq 1, \\ bx - a + b, & x \leq -1, \end{cases} \tag{2}$$

where x, y, z-phase variables, α, β, a, b-parameters ($\alpha > 0, \quad \beta > 0, \quad a < 0, \quad b < 0$). Consider

$$a = -\frac{8}{7}; \quad b = -\frac{5}{7}, \quad \alpha = 9, \quad \beta = 14. \tag{3}$$

We will replace the piecewise linear function with a cubic polynomial [22].

$$f(x) = \frac{1}{16}x^3 - \frac{7}{6}x. \tag{4}$$

The initial conditions are

$$x(0) = 0.1; \quad y(0) = 0.2; \quad z(0) = 1. \tag{5}$$

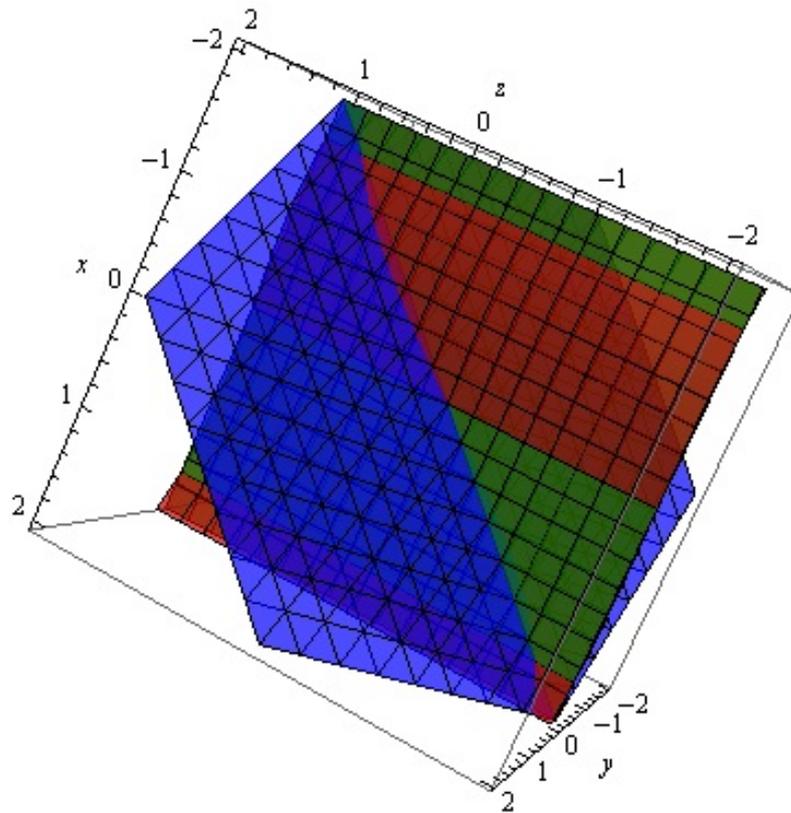The nullclines are depicted in Figure 1.

Figure 1. The visualization of nullclines for the system (1). ($x-$red, $y-$green, $z-$blue).

The system possesses precisely three critical points, determined and illustrated as the intersection points of the nullclines in Figure 1. There are three critical points at $(1.633, 0, -1.633)$, $(0, 0, 0)$ and $(-1.633, 0, 1.633)$. Linearization around these points provides us with the characteristic numbers λ. The characteristic numbers are considered in Table 1.

Table 1. Characteristic numbers.

The Critical Point	λ_1	λ_2	λ_3
$(1.633, 0, -1.633)$	-4.3563	$0.1782 - 3.1315\,i$	$0.1782 + 3.1315\,i$
$(0, 0, 0)$	2.4730	$-0.9865 - 2.7734\,i$	$-0.9865 - 2.7734\,i$
$(-1.633, 0, 1.633)$	-4.3563	$0.1782 - 3.1315\,i$	$0.1782 + 3.1315\,i$

The type of two critical points is a saddle-focus with one-dimensional stable and two-dimensional unstable manifolds. The type of critical point $(0, 0, 0)$ is a saddle-focus with two-dimensional stable and one-dimensional unstable manifolds. The chaotic attractor is depicted in Figure 2 and the graph of solutions is depicted in Figure 3.

In the equilibrium state at the origin, one root is real and positive, indicating the direction in which the initial disturbance will grow. A pair of complex conjugate roots with a negative real part signifies the presence of rotational motion and twisting of the trajectory towards a singular critical point in the plane of rotation. For each of the other two equilibrium states, the motion is unstable in the plane of rotation (the real parts of the complex conjugate pair are greater than zero). At the same time, there exists a direction in which the phase trajectory approaches the critical point.
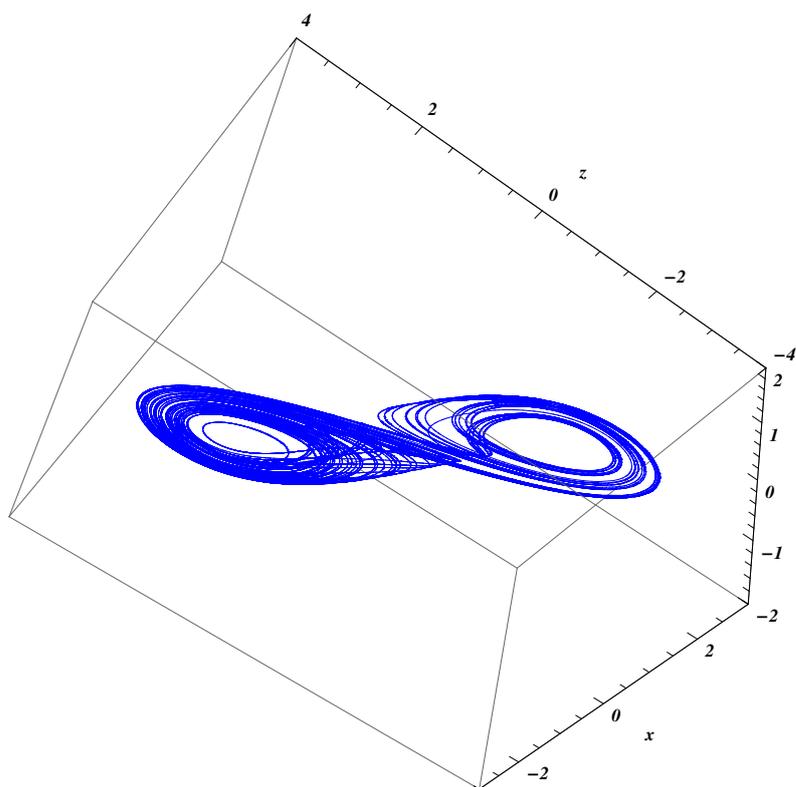
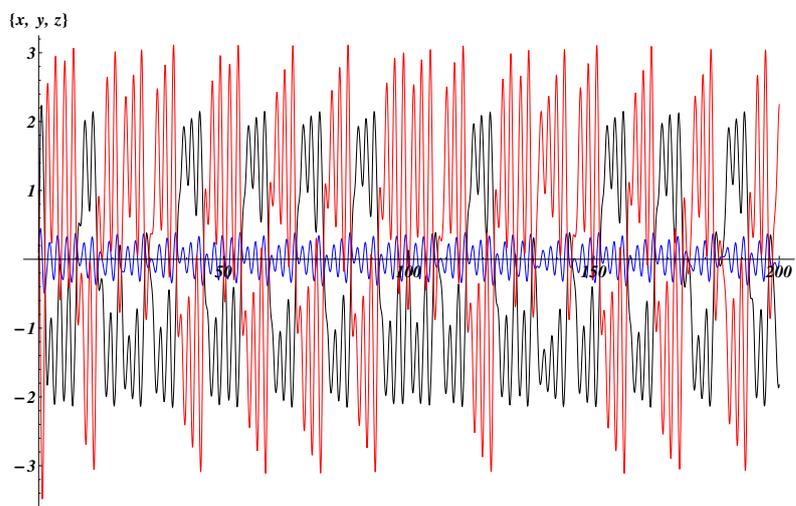**Figure 2.** Chua's double-scroll attractor: Phase portrait for the system (1).

Figure 3. Solutions (x, y, z) of the system (1) with the initial conditions $x(0) = 0.1; y(0) = 0.2; z(0) = 1$.

Lyapunov exponents after 5000 steps were $L_1 = 0.3329$, $L_2 = -0.0012$, and $L_3 = -2.9923$. The largest Lyapunov exponent was greater than 0 as shown in Figure 4.

The Lyapunov exponents characterize the exponential expansion or contraction of phase-space entities, such as one-dimensional lengths, two-dimensional areas, and three-dimensional volumes. The largest Lyapunov exponent denoted as LE_1 characterizes the average rate of divergence over time between two adjacent trajectories separated by a specific distance δ. The sum of the first n Lyapunov exponents describes the divergence or convergence rate of an n-dimensional phase-space volume [23]. The paper [24] states that the presence of at least one positive Lyapunov exponent leads to the divergence of neighboring trajectories, classifying the phase-space motion as "chaotic", but the positivity of the calculated senior Lyapunov's exponent is not the criteria of occurrence in the system

of chaotic dynamics [25,26]. The computation of the full Lyapunov exponent spectrum is a rather mathematically complicated issue. Computations are performed using Wolfram Mathematica. For Lyapunov exponents calculation the package "lce.m for Mathematica" was used [27].
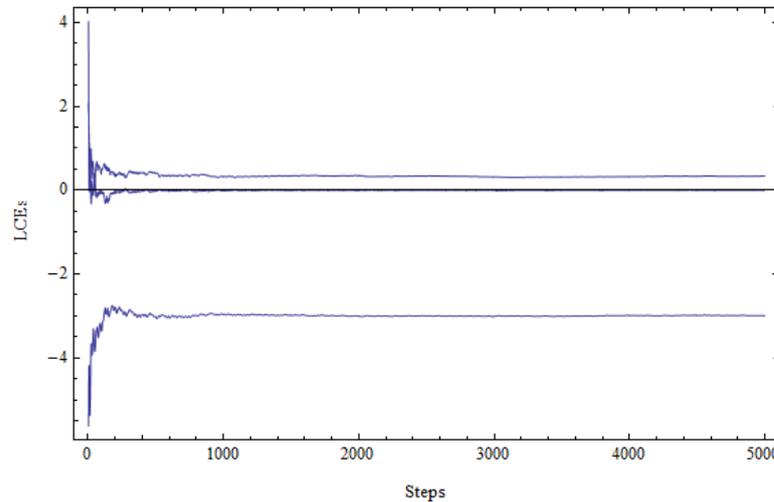

Figure 4. Lyapunov exponent spectrum of Chua circuit (1).

Meanwhile, according to the Kaplan–Yorke formula,

$$D_{KY} = j + \frac{1}{|L_{j+1}|} \sum_{i=1}^{j} L_i = 2 + \frac{L_1 + L_2}{|L_3|} = 2.1109 \tag{6}$$

the fractal dimension also further verifies that the new system has a chaotic behavior [28]. For a dissipative dynamical system, the sum of all Lyapunov exponents should equate to a negative value [29]. Only dissipative dynamical systems have attractors [30].

2.2. 3D Gene Regulatory System

Consider the system

$$\begin{cases} \dfrac{dx}{dt} = \dfrac{1}{1 + e^{-\mu_1(w_{11}x + w_{12}y + w_{13}z - \theta_1)}} - v_1 x, \\[2ex] \dfrac{dy}{dt} = \dfrac{1}{1 + e^{-\mu_2(w_{21}x + w_{22}y + w_{23}z - \theta_2)}} - v_2 y, \\[2ex] \dfrac{dz}{dt} = \dfrac{1}{1 + e^{-\mu_3(w_{31}x + w_{32}y + w_{33}z - \theta_3)}} - v_3 z, \end{cases} \tag{7}$$

where μ_i, θ_i and v_i are the parameters, w_{ij} are the coefficients of the so-called regulatory matrix

$$W = \begin{pmatrix} w_{11} & w_{12} & w_{13} \\ w_{21} & w_{22} & w_{23} \\ w_{31} & w_{32} & w_{33} \end{pmatrix}. \tag{8}$$

The parameters of the GRN have the following biological interpretations:

- v_i—degradation of the i-th gene expression product;
- w_{ij}—the connection weight or strength of control of gene j on gene i. Positive values of w_{ij} signify activating influences, whereas negative values denote repressing influences;
- θ_i—The impact of external stimuli on gene i is reflected in its ability to modulate the gene's responsiveness to activating or repressing factors [31].

The nullclines and the critical points for the system are defined by the relations

$$\begin{cases} x = \dfrac{1}{v_1} \dfrac{1}{1 + e^{-\mu_1\,(w_{11}x + w_{12}y + w_{13}z - \theta_1)}}, \\[2mm] y = \dfrac{1}{v_2} \dfrac{1}{1 + e^{-\mu_2\,(w_{21}x - w_{22}y + w_{23}z - \theta_2)}}, \\[2mm] z = \dfrac{1}{v_3} \dfrac{1}{1 + e^{-\mu_2\,(w_{21}x + w_{22}y + w_{33}z - \theta_3)}}. \end{cases}$$

The sigmoidal function $f(t) = \frac{1}{1 + e^{-\mu}}$ is used in (7). Sigmoidal functions exhibit a continuous increase from zero to one and possess a solitary inflection point. While various sigmoidal functions exist, the one mentioned above is particularly suitable for analysis and visualization [32]. Such systems were considered in [20,33–35].

2.3. Linearized System

The linearized system for any critical point (x^*, y^*, z^*)

$$\begin{cases} u_1' = -v_1 u_1 + \mu_1 w_{11} g_1 u_1 + \mu_1 w_{12} g_1 u_2 + \mu_1 w_{13} g_1 u_3, \\ u_2' = -v_2 u_2 + \mu_2 w_{21} g_2 u_1 + \mu_2 w_{22} g_2 u_2 + \mu_2 w_{23} g_2 u_3, \\ u_3' = -v_3 u_3 + \mu_3 w_{31} g_3 u_1 + \mu_3 w_{32} g_3 u_2 + \mu_3 w_{33} g_3 u_3, \end{cases}$$

where

$$g_1 = \frac{e^{-\mu_1(w_{11}x^* + w_{12}y^* + w_{13}z^* - \theta_1)}}{\left[1 + e^{-\mu_1(w_{11}x^* + w_{12}y^* + w_{13}z^* - \theta_1)}\right]^2}, \tag{9}$$

$$g_2 = \frac{e^{-\mu_2(w_{21}x^* + w_{22}y^* + w_{23}z^* - \theta_2)}}{\left[1 + e^{-\mu_2(w_{21}x^* + w_{22}y^* + w_{23}z^* - \theta_2)}\right]^2}, \tag{10}$$

$$g_3 = \frac{e^{-\mu_3(w_{31}x^* + w_{32}y^* + w_{33}z^* - \theta_3)}}{\left[1 + e^{-\mu_3(w_{31}x^* + w_{32}y^* + w_{33}z^* - \theta_3)}\right]^2}. \tag{11}$$

One has

$$A - \lambda I = \begin{vmatrix} \mu_1 w_{11} g_1 - v_1 - \lambda & \mu_1 w_{12} g_1 & \mu_1 w_{13} g_1 \\ \mu_2 w_{21} g_2 & \mu_2 w_{22} g_2 - v_2 - \lambda & \mu_2 w_{23} g_2 \\ \mu_3 w_{31} g_3 & \mu_3 w_{32} g_3 & \mu_3 w_{33} g_3 - v_3 - \lambda \end{vmatrix}$$

and the characteristic equation is

$$\det|A - \lambda I| = -\lambda^3 + \lambda^2(-v_1 - v_2 - v_3 + \mu_1 w_{11} g_1 + \mu_2 w_{22} g_2 + \mu_3 w_{33} g_3) + \lambda(g_1 v_3 \mu_1 w_{11} +$$

$$+ \mu_2 w_{22} g_2 v_3 + g_1 g_2 w_{21} \mu_1 \mu_2 w_{12} - g_1 g_2 w_{11} w_{22} \mu_1 \mu_2 + g_1 g_3 w_{31} w_{13} \mu_1 \mu_3 -$$

$$- g_1 g_3 w_{11} w_{33} \mu_1 \mu_3 + g_2 g_3 w_{32} w_{23} \mu_2 \mu_3 - g_2 g_3 w_{22} w_{33} \mu_2 \mu_3 - v_1(v_2 + v_3 - g_2 w_{22} \mu_2 - g_3 w_{33} \mu_3) +$$

$$+ v_2(-v_3 + g_1 w_{11} \mu_1 + g_3 w_{33} \mu_3)) + v_1(v_2(-v_3 + g_3 w_{33} \mu_3) + g_2 \mu_2(v_3 w_{22} + g_3 w_{32} w_{23} \mu_3 -$$

$$g_3 w_{22} w_{33} \mu_3)) + g_1 \mu_3(v_2(v_3 w_{11} + g_3(w_{31} w_{13} - w_{11} w_{33})\mu_3) + g_2 \mu_2(v_3(w_{21} w_{12} - w_{11} w_{22}) +$$

$$+ g_3(-w_{31} w_{22} w_{13} + w_{21} w_{32}\,w_{13} + w_{31} w_{12} w_{23} - w_{11} w_{32}\,w_{23} - w_{21} w_{12} w_{33} + w_{11} w_{22}\,w_{33})\mu_3)) = 0.$$

The characteristic equation can be rewritten as

$$-\lambda^3 + A\lambda^2 + B\lambda + C = 0, \tag{12}$$

where

$$A = -(v_1 + v_2 + v_3) + g_1 w_{11} \mu_1 + g_2 w_{22} \mu_2 + g_3 w_{33} \mu_3,$$

$$
\begin{aligned}
B &= \mu_1\mu_2 w_{31} w_{13} g_1 g_3 - \mu_2\mu_3 w_{32} w_{23} g_2 g_3 + \mu_1\mu_2 w_{21} w_{12} g_1 g_2 \\
&\quad - (\mu_2 w_{22} g_2 - v_2)(\mu_3 w_{33} g_3 - v_3) - (\mu_1 w_{11} g_1 - v_1)(\mu_3 w_{33} g_3 - v_3) \\
&\quad - (\mu_1 w_{11} g_1 - v_1)(\mu_2 w_{22} g_2 - v_2),
\end{aligned}
$$

$$
\begin{aligned}
C &= (\mu_1 w_{11} g_1 - v_1)(\mu_2 w_{22} g_2 - v_2)(\mu_3 w_{33} g_3 - v_3) + \mu_1\mu_2\mu_3 w_{21} w_{32} w_{23} g_1 g_2 g_3 \\
&\quad + \mu_1\mu_2\mu_3 w_{31} w_{12} w_{23} g_1 g_2 g_3 - \mu_1\mu_3 w_{31} w_{13} g_1 g_3 (\mu_2 w_{22} g_2 - v_2) \\
&\quad - \mu_2\mu_3 w_{32} w_{23} g_2 g_3 (\mu_1 w_{11} g_1 - v_1) - \mu_1\mu_2 w_{21} w_{12} g_1 g_2 (\mu_3 w_{33} g_3 - v_3).
\end{aligned}
$$

Theorem 1. *The vector field* $(f_1(x,y,z), f_2(x,y,z), f_3(x,y,z))$, *where* f_1, f_2 *and* f_3 *are the right sides of the equations in* (7), *is directed inward on the boundary of the domain* $Q_3 := \{(x,y,z) : 0 < x < \frac{1}{v_1}, 0 < y < \frac{1}{v_2}, 0 < z < \frac{1}{v_3}\}$.

Proof of Theorem 1. Take one of faces of the parallelepiped Q_3, for example, $x = 0$. The vector field there in the x direction is $f_1 - v_1, x = f > 0$. Take face $x = \dfrac{1}{v_1}$. The vector field in the x direction is $f_1 - v_1, x = f_1 - v_1, \dfrac{1}{v_1} = f_1 - 1 < 0$. In both cases, the vector field along the x axis is directed inside Q_3. Similarly, other faces of Q_3 can be considered. $\square$

Theorem 2. *System* (7) *has at least one equilibrium (critical point). All equilibria are located in the open box* $Q_3 := \{(x,y,z) : 0 < x < \frac{1}{v_1}, 0 < y < \frac{1}{v_2}, 0 < z < \frac{1}{v_3}\}$.

This follows from the result of the mapping of a topological ball into itself. The second assertion follows from the fact that nullclines meet and can intersect only in Q_3.

3. Results

3.1. 3D Chaotic Attractor

The system (7) with the matrix

$$
W = \begin{pmatrix}
0.06 & -0.825 & 0.19 \\
1.915 & 1.76 & -0.32 \\
3.7 & 0.128 & 0.985
\end{pmatrix}
\tag{13}
$$

and $\mu_1 = 4, \mu_2 = 5.02, \mu_3 = 8, v_1 = v_2 = v_3 = 1$ and

$$
\theta_1 = \frac{w_{11} + w_{12} + w_{13}}{2},
$$

$$
\theta_2 = \frac{w_{21} + w_{22} + w_{23}}{2},
$$

$$
\theta_3 = \frac{w_{31} + w_{32} + w_{33}}{2}
$$

has three critical points. Linearization around these points provides us with the characteristic numbers λ.

The initial conditions are

$$
x(0) = 0.592; \quad y(0) = 0.85; \quad z(0) = 2.
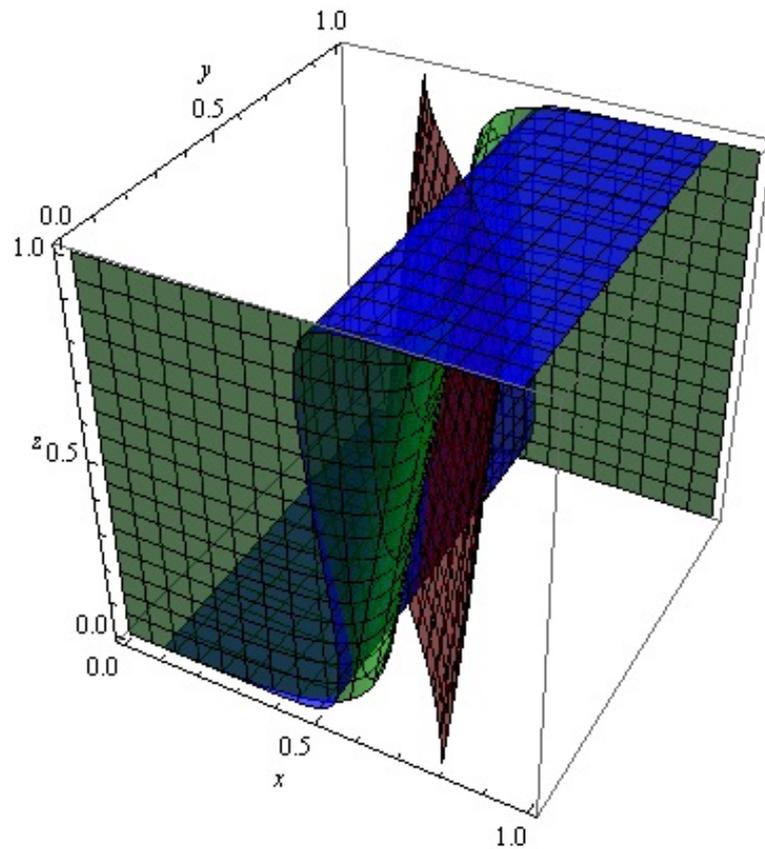\tag{14}
$$

The nullclines are depicted in Figure 5.

Figure 5. Nullclines x_1—red, x_2—green, x_3—blue of the system (7) with the regulatory matrix (13).

The characteristic equation for critical points is (12). The coefficients of characteristic Equation (12) are considered in Table 2.

Table 2. Coefficients of characteristic Equation (12).

The Critical Point	A	B	C
$(0.4398, 0.4545, 0.0032)$	-0.725248	-0.557956	-0.787449
$(0.5, 0.5, 0.5)$	1.2388	0.195983	1.59353
$(0.5602, 0.5455, 0.9968)$	-0.725248	-0.557956	-0.787449

Characteristic numbers are considered in Table 3.

Table 3. Characteristic numbers.

The Critical Point	λ_1	λ_2	λ_3
$(0.4398, 0.4545, 0.0032)$	-0.9780	$0.12638 - 0.888361\,i$	$0.12638 + 0.888361\,i$
$(0.5, 0.5, 0.5)$	1.82477	$-0.292985 - 0.887376\,i$	$-0.292985 + 0.887376\,i$
$(0.5602, 0.5455, 0.9968)$	-0.9780	$0.12638 - 0.888361\,i$	$0.12638 + 0.888361\,i$

The type of two critical points is a saddle-focus with one-dimensional stable and two-dimensional unstable manifolds. The type of critical point $(0.5, 0.5, 0.5)$ is a saddle-focus with two-dimensional stable and one-dimensional unstable manifolds. The chaotic attractor is depicted in Figures 6 and 7. The graph of solutions is depicted in Figures 8 and 9.
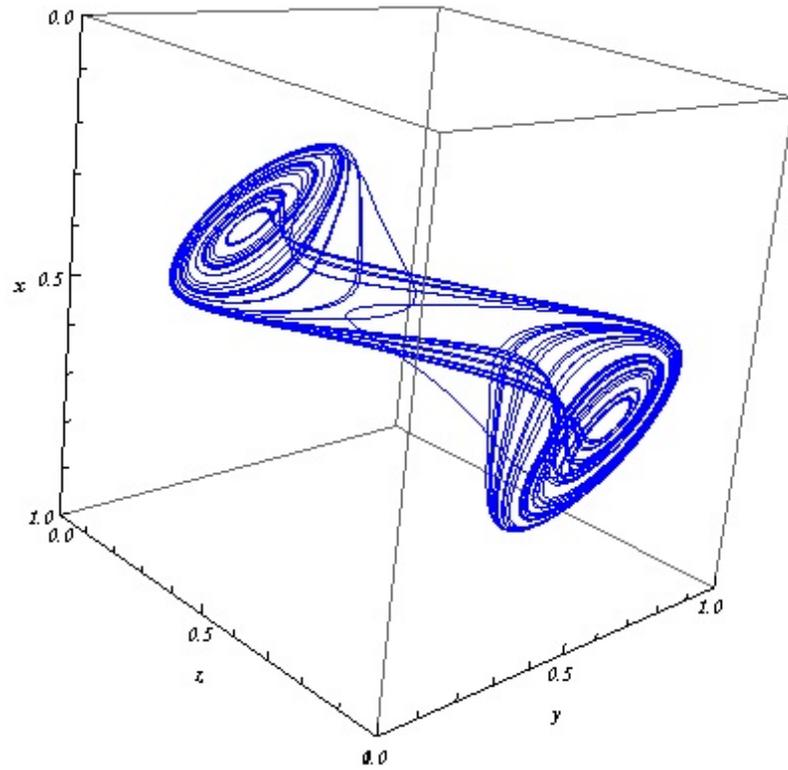
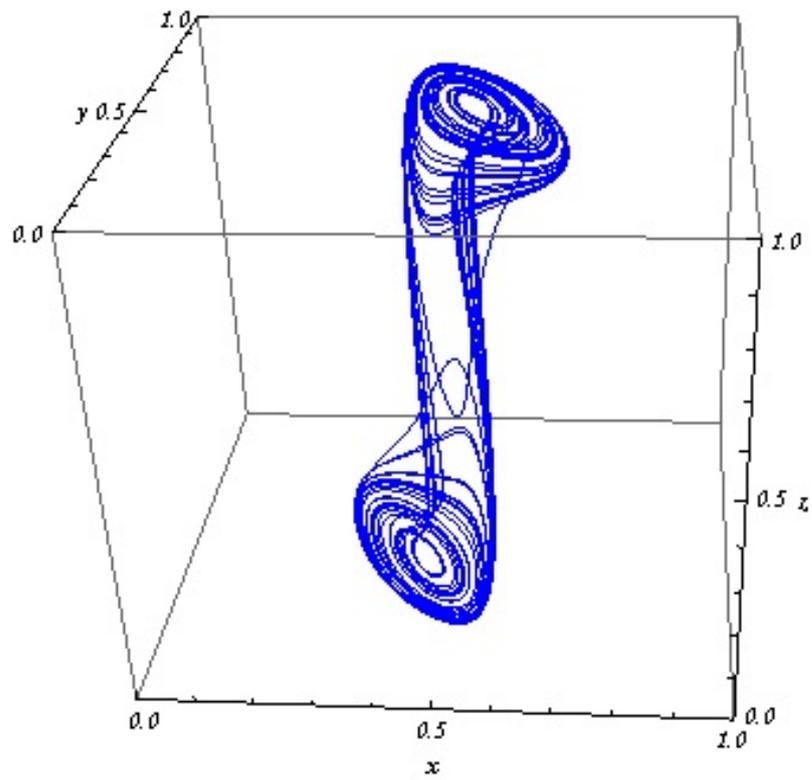**Figure 6.** The visualization of chaotic attractor of the system (7) with the regulatory matrix (13).

Figure 7. The visualization of chaotic attractor of the system (7) with the regulatory matrix (13), other view.
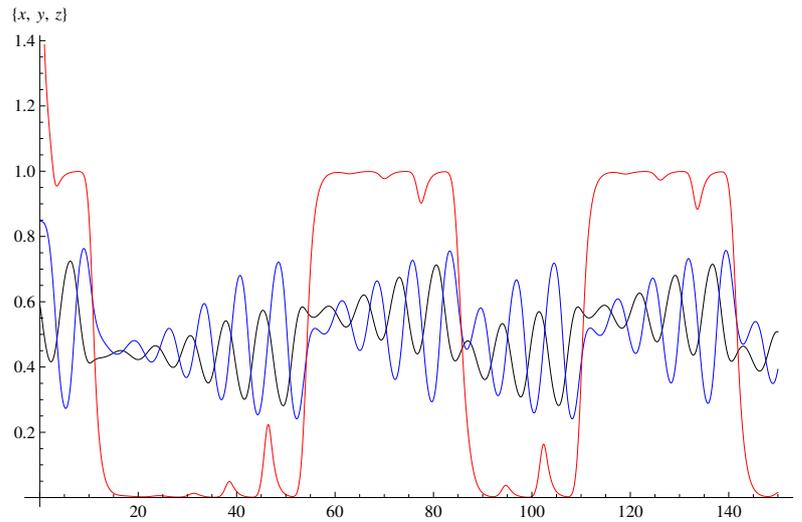
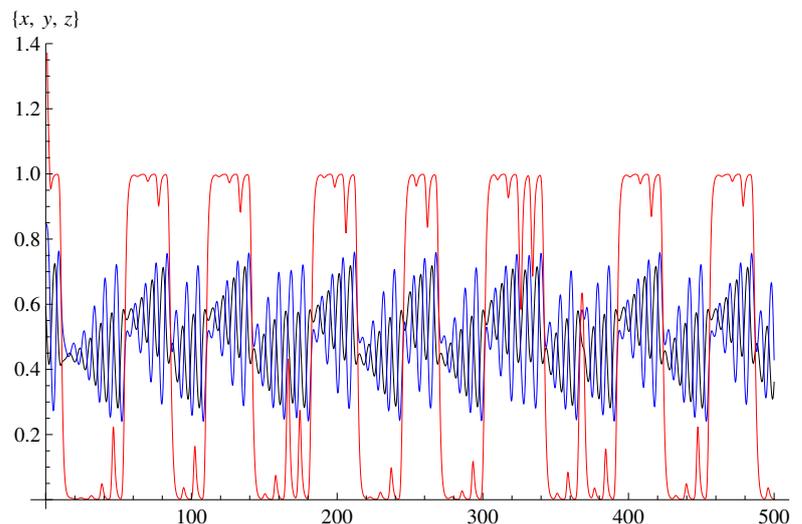**Figure 8.** Solutions (x, y, z) of the system (7) with the regulatory matrix (13).

Figure 9. Solutions (x, y, z) of the system (7) with the regulatory matrix (13).

Lyapunov exponents after 5000 steps were $L_1 = 0.0398$, $L_2 = -0.0026$ and $L_3 = -0.7665$. The largest Lyapunov exponent was greater than 0 as shown in Figure 10.
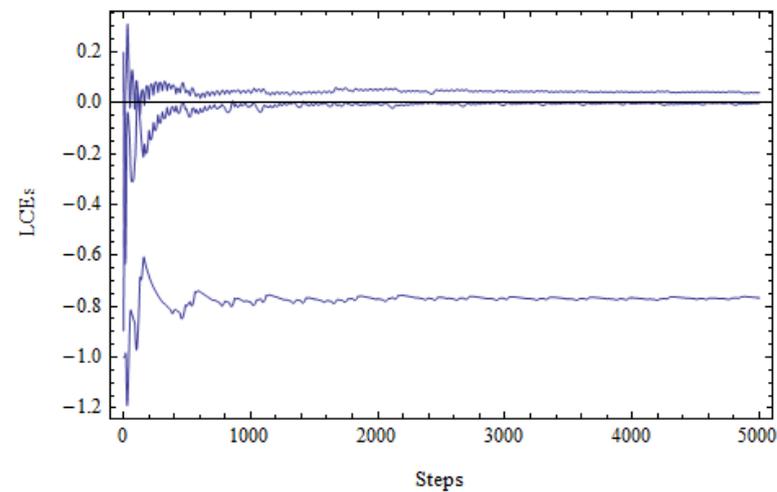

Figure 10. Lyapunov exponent of the system (7) with the regulatory matrix (13).

3.2. Bifurcation

The bifurcation theory of differential equation systems, first introduced in the works of Jules Henri Poincare (1854–1912), elucidates qualitative, abrupt alterations in the phase portraits of these systems as their parameters undergo continuous and smooth changes [36]. We take w_{23} as a bifurcation parameter (that is, the third element in the second row) in the regulatory matrix (13). Computations are performed using Wolfram Mathematica. Results of calculations for the system (7) with regulatory matrix (13), changing the parameter w_{23}. are considered in Table 4.

Table 4. Results of calculations for the system (7) with regulatory matrix (13), changing the parameter w_{23}.

w_{23}	x^*, y^*, z^*	λ_1	λ_2	λ_3
	(0.2673, 0.6735, 0.00002)	−0.9998	−0.0051 − 0.6838 i	−0.0051 − 0.6838 i
−0.569	(0.5, 0.5, 0.5)	2.0836	−0.4224 − 1.2107 i	−0.4224 + 1.2107 i
	(0.7327, 0.3265, 0.99998)	−0.9998	−0.0051 − 0.6838 i	−0.0051 + 0.6838 i
	(0.3190, 0.6015, 0.0001)	−0.9990	0.0849 − 0.7646 i	0.0849 + 0.7646 i
−0.5	(0.5, 0.5, 0.5)	−0.3913	−0.3913 − 1.1361	−0.3913 + 1.1361
	(0.6810, 0.3985, 0.9999)	−0.9990	0.0849 − 0.7646 i	0.0849 + 0.7646 i
	(0.3885, 0.5144, 0.0007)	−0.9941	0.1319 − 0.8505 i	0.1319 + 0.8505 i
−0.4	(0.5, 0.5, 0.5)	1.9197	−0.3404 − 1.0104 i	−0.3404 + 1.0104 i
	(0.6115, 0.4856, 0.9993)	−0.9941	0.1319 − 0.8505 i	0.1319 + 0.8505 i
	(0.4521, 0.4406, 0.0046)	−0.9698	0.1214 − 0.8932 i	0.1214 + 0.8932 i
−0.3	(0.5, 0.5, 0.5)	1.7985	−0.2799 − 0.8520 i	−0.2799 + 0.8520 i
	(0.5479, 0.5594, 0.9954)	−0.9698	0.1214 − 0.8932 i	0.1214 + 0.8932 i
	(0.4873, 0.4023, 0.0133)	−0.9247	0.1061 − 0.8937 i	0.1061 + 0.8937 i
−0.241	(0.5, 0.5, 0.5)	1.7130	−0.2371 − 0.7312 i	−0.2371 + 0.7312 i
	(0.5127, 0.5977, 0.9868)	−0.9247	0.1061 − 0.8937 i	0.1061 + 0.8937 i
	(0.4879, 0.4017, 0.0135)	−0.9235	0.1059 − 0.8935 i	0.1059 + 0.8935 i
−0.24	(0.5, 0.5, 0.5)	1.7114	−0.2363 − 0.7289 i	−0.2363 + 0.7289 i
	(0.5121, 0.5983, 0.9865)	−0.9235	0.1059 − 0.8935 i	0.1059 + 0.8935 i
0	(0.5, 0.5, 0.5)	−0.7071	0.9729 − 0.3612 i	0.9729 + 0.3612 i
8	(0.5, 0.5, 0.5)	−3.7550	2.4969 − 3.1062 i	2.4969 + 3.1062 i

Lyapunov exponents are considered in Table 5.

Table 5. Lyapunov exponents.

w_{23}	LE_1	LE_2	LE_3
−0.569	−0.0106	−0.0149	−0.9997
−0.5	−0.00002	−0.1529	−0.9907
−0.4	0.0026	−0.2235	−0.8975
−0.3	0.0309	−0.0127	−0.7389
−0.241	0.0512	−0.0062	−0.6901
−0.24	0.0020	−0.0260	−0.7109
0	−0.0029	−0.6131	−0.9340
8	0.0016	−0.9139	−1.5327

Periodic attractors are depicted in Figures 11–13. Graphs of solutions are depicted in Figures 14–16. The chaotic attractor is depicted in Figure 17 and the graph of solutions is depicted in Figure 18.
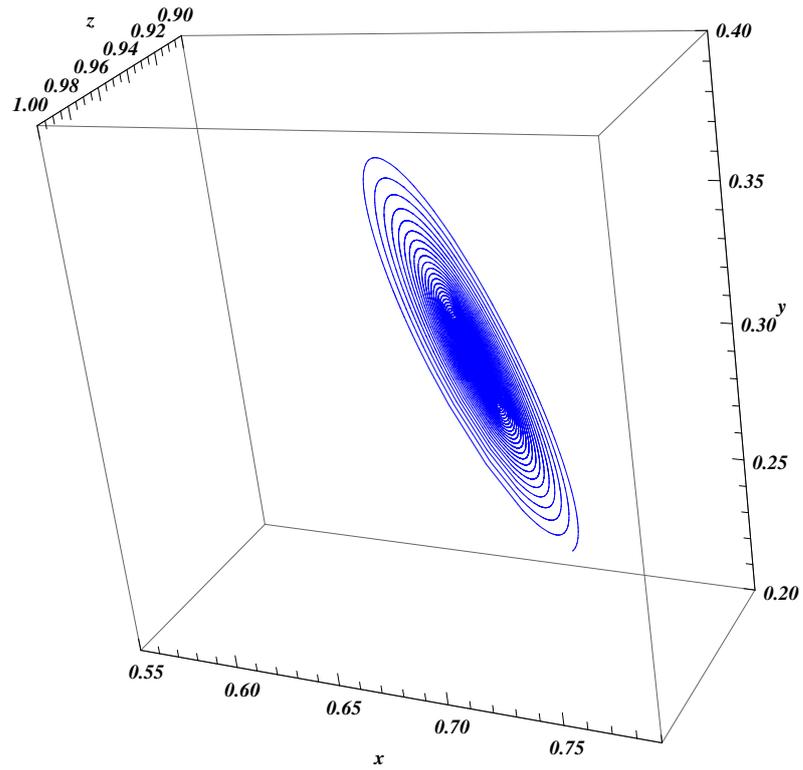
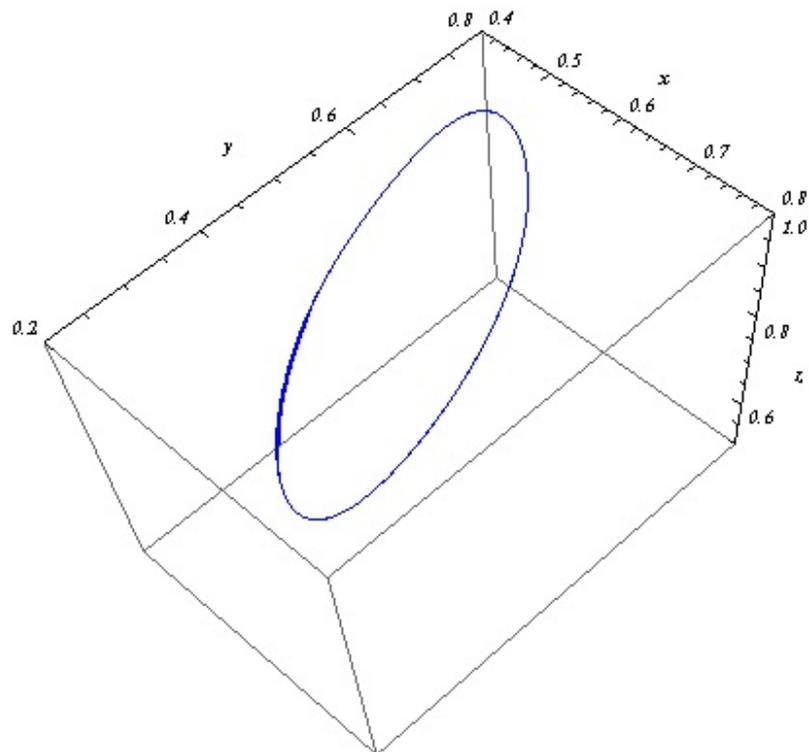**Figure 11.** The visualization of the periodic attractor, $w_{23} = -0.569$.

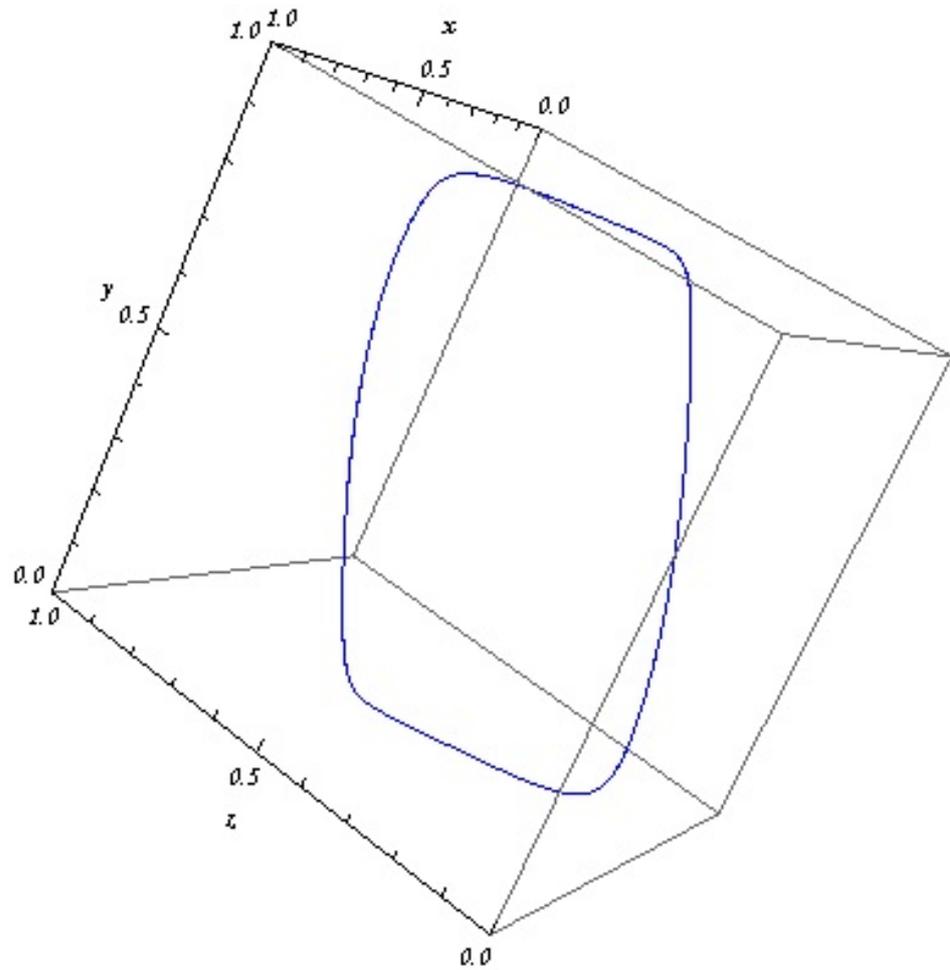**Figure 12.** The visualization of the periodic attractor, $w_{23} = -0.4$.

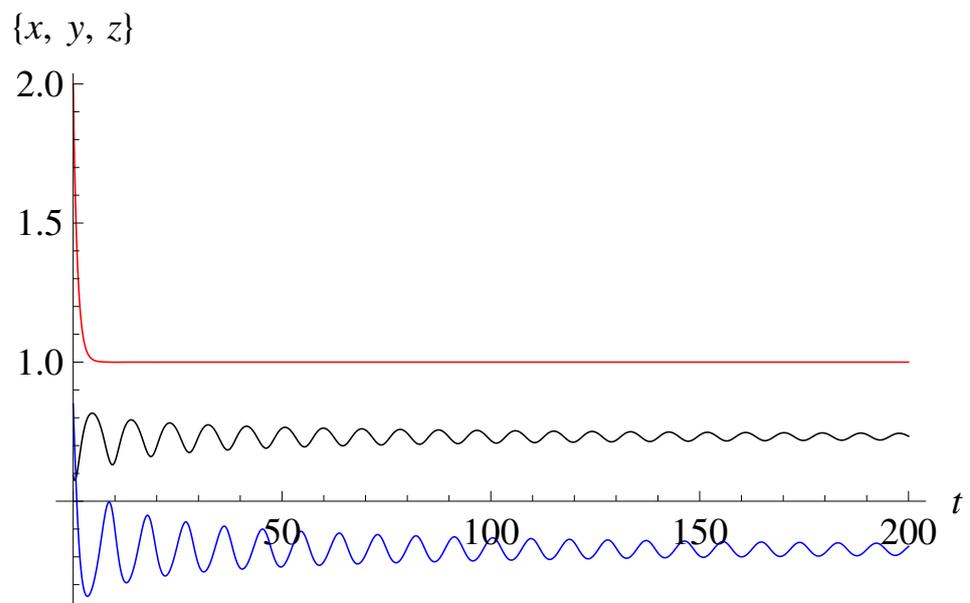**Figure 13.** The visualization of the periodic attractor, $w_{23} = 8$.

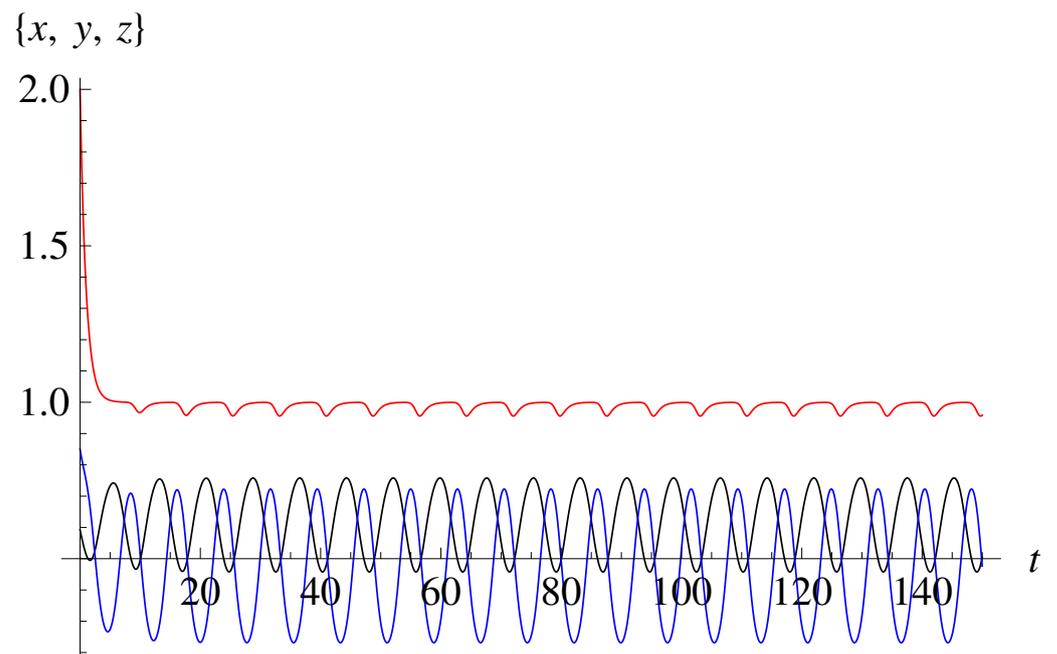**Figure 14.** Solutions (x, y, z) of the system (7) with the regulatory matrix (13), $w_{23} = -0.569$.

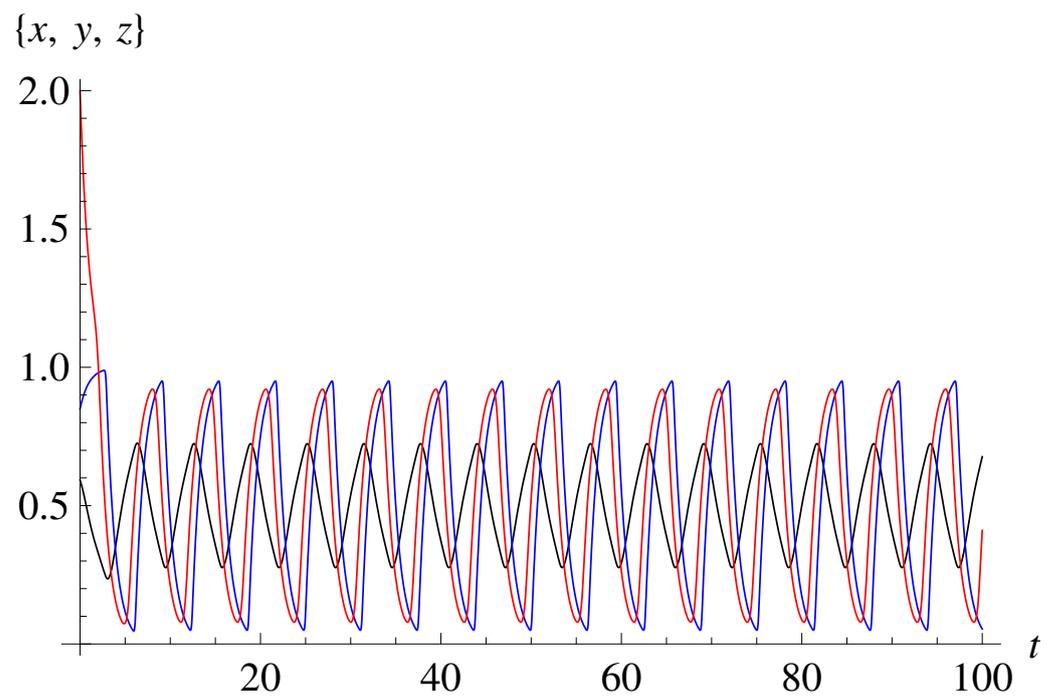**Figure 15.** Solutions (x, y, z) of the system (7) with the regulatory matrix (13), $w_{23} = -0.4$.

Figure 16. Solutions (x, y, z) of the system (7) with the regulatory matrix (13), $w_{23} = 8$.
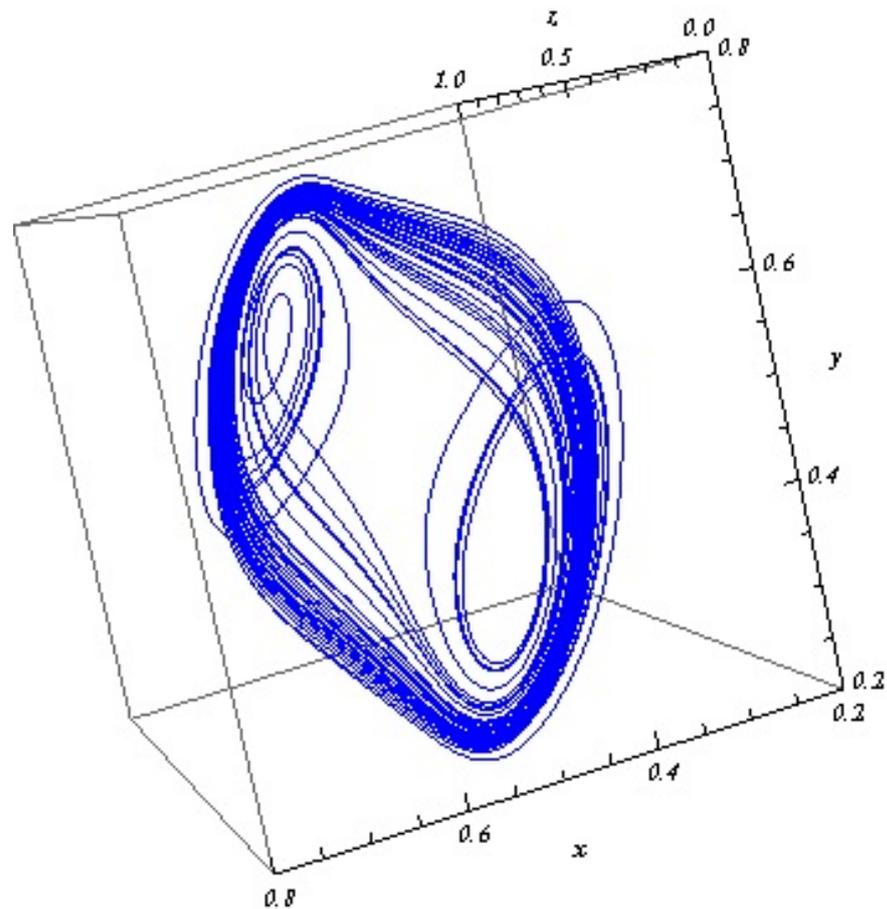
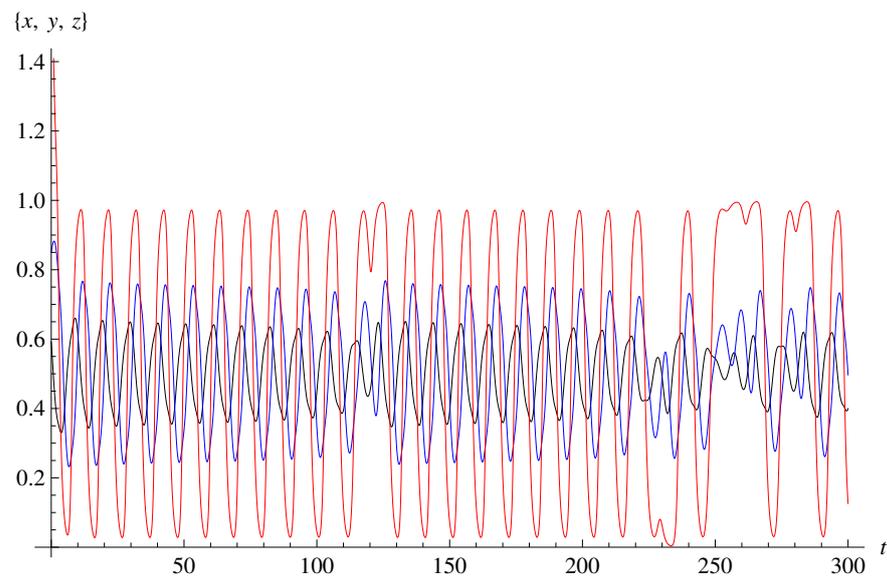**Figure 17.** The visualization of the chaotic attractor, $w_{23} = -0.2401$.

Figure 18. Solutions (x, y, z) of the system (7) with the regulatory matrix (13), $w_{23} = -0.2401$.

4. Discussion

A definite similarity was found between the Chua circuits and systems of the form (7), which are used in the mathematical modeling of genetic and neuronal networks. An analysis of critical points and their mutual positions in the Chua system motivated us to study similar configurations in GRN systems. The local analysis of critical points gave hints of

what should be arranged in GRN systems to get similar behavior of trajectories as in the Chua system. For this, multiple parameters, built into GRN systems, were useful. The desired behavior can be reached by shifting the nullclines, changing θ parameters, or/and changing the elements of the regulatory matrix, and regulating the form of sigmoidal functions by changing μ parameters. Looking at the data being collected during the study, one may observe some properties that eventually lead to chaotic behavior. As an example, Tables 1–3 with the local characteristics of the critical points, should be mentioned. The bifurcation analysis made in the article concerns the varying of one parameter. The changes in the characteristics of critical points and fractal dimensionality of the chaotic attractor, give rise to conclusions and may indicate directions of further numerical experiments. Some questions arise. For instance, the monotone change in the parameter w_{23} leads to generally non-monotone changes in characteristics of the critical points and KY fractal dimensionalities of the chaotic attractor. Analyzing the collected data may lead to the formulation of directions for further studies. The questions that should be answered: what is the minimal (or optimal) number of critical points needed for the birth of a strange attractor; what is the minimal configuration (positions, local characteristics) that ensures a transition to chaotic behavior; is the transition to chaotic behavior in the studied system possible without passing through the stable periodic solution stage; could sufficient conditions be formulated to ensure passage to chaotic behavior from a given configuration; what is the description of this configuration; what are the necessary conditions concerning passage to chaotic behavior; is it possible to pass from periodic attractors to chaotic ones through continuous change of KY dimensionality; generally, what is the role of jump changes in a system to go to the strange (chaotic) attractor?

This list can be continued and answering some, or all, of the formulated questions concerning the system (7) (with matrix (13), at least) would indicate the essential progress in understanding the process of formation of a chaotic attractor. So further investigations in this direction promise results, which may be relevant and important for the general theory of dynamical systems.

Author Contributions: Conceptualization, F.S.; methodology, O.K. and I.S.; software, O.K. and I.S.; formal analysis, O.K. and F.S.; investigation, O.K.; resources, I.S.; data curation, I.S. and F.S.; writing—original draft preparation, I.S. and O.K.; writing—review and editing, I.S. and F.S.; visualization, O.K.; supervision, I.S.; project administration, I.S.; funding acquisition, O.K. All authors have read and agreed to the published version of the manuscript.

Data Availability Statement: Data were created or analyzed in this study.

Abbreviations

The following abbreviations are used in this manuscript:

GRN   Gene regulatory network

References

1. Ramar, R. Design of a New Chaotic System with Sine Function: Dynamic Analysis and Offset Boosting Control. *Chaos Theory Appl.* **2023**, *5*, 118–126. [CrossRef]
2. Mansour, M.; Donmez, T.B.; Kutlu, M.C.; Freeman, C. Respiratory Diseases Prediction from a Novel Chaotic System. *Chaos Theory Appl.* **2023**, *5*, 20–26. [CrossRef]
3. Keles, Z.; Sonugur, G.; Alcn, M. The Modeling of the Rucklidge Chaotic System with Artificial Neural Networks. *Chaos Theory Appl.* **2023**, *5*, 59–64. [CrossRef]
4. Jorgensen, S.E. *Encyclopedia of Ecology*; Elsevier: Amsterdam, The Netherlands, 2008.

5. Ibrahim, K.M.; Jamal, R.K.; Ali, F.H. Chaotic behaviour of the Rossler model and its analysis by using bifurcations of limit cycles and chaotic attractors. *J. Phys. Conf. Ser.* **2018**, *1003*, 012099. [CrossRef]

6. Xiyin, L.; Guoyuan, Q. Mechanical analysis of Chen chaotic system. *Chaos Solitons Fractals* **2017**, *98*, 173–177. [CrossRef]

7. Lu, J.; Chen, G.; Guoyuan, Q. A new chaotic attractor coined. *Int. J. Bifurc. Chaos* **2002**, *12*, 659–661. [CrossRef]

8. Mota, M.C.; Oliveira., R.D.S.; Qi, G. Dynamic aspects of Sprott BC chaotic system. *Discret. Contin. Syst.* **2021**, *26*, 1653–1673. [CrossRef]

9. Kazuyuki, A. Chaos and Its Applications. *Procedia IUTAM* **2012**, *5*, 199–203. [CrossRef]

10. Ott, E. *Chaos in Dynamical Systems*, 2nd ed.; Cambridge University Press: London, UK, 2002. [CrossRef]

11. Feier, S. The Chaos Theory and its Application. *J. Phys. Conf. Ser.* **2012**, *012118*, 2021.

12. Klioutchnikov, I.; Sigova, M.; Beizerov, N. Chaos Theory in Finance. *Procedia Comput. Sci.* **2017**, *2017*, 368–375. [CrossRef]

13. Biswas, H.R.; Hasan, M.M.; Bala, S.K. Chaos theory and its applications in our real life. *Barishal Univ. J.* **2018**, *5*, 123–140.

14. Joan, P.; Dandoy, R. Chaos theory and its application in political science. In Proceedings of the IPSA World Congress, Fukuoka, Japan, 9–13 July 2006 .

15. May, M.R. Chaos and the dynamics of biological populations. *Nucl. Proc. Suppl.* **1987**, *2*, 225–245. [CrossRef]

16. Zang, X.; Iqbal, S.; Zhu, Y.; Liu, X.; Zhao, J. Applications of Chaotic Dynamics in Robotics. *Int. J. Adv. Robot.* **2016**, *13* . [CrossRef]

17. Rana, S.M.S. Bifurcation Analysis and 0–1 Chaos Test of a Discrete T System. *Chaos Theory Appl.* **2023**, *5*, 90–104. [CrossRef]

18. Lynch, S.E. *Dynamical Systems with Applications Using Mathematica*; Springer: Cham, Switzerland, 2017

19. Hastings, A.; Hom, C.L.; Ellner, S.; Turchin, P.; Godfray, H.C.J. Chaos in Ecology: Is Mother Nature a Strange Attractor? *Annu. Rev. Ecol. Syst.* **1993**, *24*, 1–33. [CrossRef]

20. Samuilik, I.; Sadyrbaev, F.; Ogorelova, D. Comparative Analysis of Models of Gene and Neural Networks. *Contemp. Math.* **2023**, *4*, 217–229. [CrossRef]

21. Bugajevskij, M.; Ponomarenko, V. *Study of Chua Circuit Behavior*; Fundamental and Comparative Research; Saratov State University: Saratov, Russia, 1999.

22. Pavlov, A.N. *Study of Chua Generator Dynamics Modes*; Saratov State University: Saratov, Russia, 2006; pp. 1–13.

23. Syed Ali, M.; Vadivel, R. Decentralized Event-Triggered Exponential Stability for Uncertain Delayed Genetic Regulatory Networks with Markov Jump Parameters and Distributed Delays. *Neural Process. Lett.* **2018**, *47*, 1219–1252. [CrossRef]

24. Hoover, W.G.; Tull, C.G.; Posch, H. Negative Lyapunov exponents for dissipative systems. *Phys. Lett. A* **1998**, *131*, 211–215. [CrossRef]

25. Magnitskii, N.A. Universal Bifurcation Chaos Theory and Its New Applications. *Mathematics* **2023**, *11*, 2536. [CrossRef]

26. Magnitskii, N.A. Bifurcation Theory of Dynamical Chaos. In *Chaos Theory*; IntechOpen: Rijeka, Croatia, 2018.

27. Software. Available online: www.msandri.it/soft.html (accessed on 21 September 2023).

28. Wang, J.; Dong, C.; Li, H. A New Variable-Boostable 3D Chaotic System with Hidden and Coexisting Attractors: Dynamical Analysis, Periodic Orbit Coding, Circuit Simulation, and Synchronization. *Fractal Fract.* **2022**, *6*, 740. [CrossRef]

29. Sayed, W.S.; Radwan, A.G.; Fahmy, H.A.A. Chaos and Bifurcation in Controllable Jerk-Based chaotic Attractors. In *Nonlinear Dynamical Systems with chaotic and Hidden Attractors*; Springer: Cham, Switzerland, 2018; pp. 45–70.

30. Nikolov, S.; Nedkova N. Gyrostat Model Regular And Chaotic Behavior. *J. Theor. Appl. Mech.* **2015**, *45*, 15–30. [CrossRef]

31. Vijesh, N.; Kumar, S.; Sreekumar, C.J. Modelling three dimensional gene regulatory networks. *WSEAS Trans. Syst. Control* **2021**, *16*, 755–763. [CrossRef]

32. Ogorelova, D.; Sadyrbaev, F.; Samuilik, I. On Targeted Control over Trajectories of Dynamical Systems Arising in Models of Complex Networks. *Mathematics* **2023**, *11*, 2206. [CrossRef]

33. Samuilik, I.; Sadyrbaev, F. On trajectories of a system modeling evolution of genetic networks. *Math. Biosci. Eng.* **2023**, *20*, 2232–2242. [CrossRef]

34. Vijesh, N.; Chakrabarti, S.; Sreekumar, J. Modeling of gene regulatory networks: A review. *J. Biomed. Sci. Eng.* **2013**, *6*, 223–231. [CrossRef]

35. Kozlovska, O.; Sadyrbaev, F. On attractors in systems of ordinary differential equations arising in models of genetic networks. *Vibroeng. Procedia* **2023**, *49*, 136–140. [CrossRef]

36. Magnitskii, N.A.; Sidorov, S.V. *New Methods for Chaotic Dynamics*; World Scientific: Singapore, 2006; pp. 1–384. [CrossRef]